Full Paper
doi.org/10.1002/ejic.202000750

Rhenium Complexes

Reactions of Schiff Base-Substituted Diselenides and -tellurides with Ni(II), Pd(II) and Pt(II) Phosphine Complexes

Maximilian Roca Jungfer,[a] Ernesto Schulz Lang,[b] and Ulrich Abram*[a]

Abstract: The salicylidene Schiff bases of bis(2-aminophenyl)diselenide and -ditelluride react with $[M^{II}Cl_2(PPh_3)_2]$ (M = Ni, Pt) or $[Pd^{II}(OAc)_2(PPh_3)_2]$ with formation of square-planar complexes with the general formulae $[M^{II}(L^Y)(PPh_3)]$ (M = Ni, Pd, Pt, Y = Se, Te). The ligands coordinate to the metals as tridentate {O,N,Se/Te} chelates. The reduction of the dichalcogenides and the formation of the chalcogenolato ligands occurs in situ by released PPh_3 ligands. A mechanism for such reactions has been derived from the experimental data with the aid of DFT calculations. It suggests a higher polarization of the dichalcogenide bond with partial charge separation upon coordination to a metal centre, which therefore facilitates the cleavage of the dichalcogenide bond with PPh_3. In accordance with the proposed mechanism, best yields are obtained with a strict exclusion of oxygen, but in the presence of water.

Introduction

The interest in the chemistry of the nickel, palladium and platinum triad is fueled by the manifold of catalytic properties of their complexes and their biological activities. Many easily accessible chelating ligand systems were exhaustively investigated in this regard. Until today, tri- and tetradentate Schiff bases are common ligands for nickel, palladium and platinum, as they yield stable, flexible and easily tunable complexes due to the modularity of the Schiff base preparation.[1–15] Hundreds of such compounds have been characterized crystallographically.[16] The introduction of additional chalcogen donor atoms in the form of arylchalcogenolato units is a common motif to modulate the properties of the resulting complexes.[1,4–15] However, only a few of such complexes with aryltellurolato ligands have been structurally characterized up to now.[16] More complexes are known with arylselenolato ligands, albeit mainly derived from simple diphenyldiselenide and still with very limited accessibility compared to their sulfur and oxygen analogs. The synthesis of the arylselenolato and -tellurolato ligands is commonly complicated in contrast to the corresponding phenolato and thiophenolato ligands because the respective selenols and tellurols are unstable. They are commonly prepared by the reduction of the corresponding diorganodichalcogenides directly before the complex formation. The reaction conditions of such procedures must be controlled carefully in order to avoid the parallel reduction of the transition metal ions.[17,18] Occasionally, nickel, palladium and platinum complexes with organochalcogenolato ligands have been prepared from the dichalcogenides via an oxidative addition to a low-valent metal species.[19–23] In the case of palladium, organochalcogenolato complexes are also accessible via an oxidative addition to Pd^{II} with formation of Pd^{IV} species. But often complex mixtures and mainly polynuclear complexes are obtained following such procedures.[24–29] Overall, the methods for the preparation of complexes with heavier chalcogenolates as ligands remain limited.

Recently, we reported an alternative method for the preparation of rhenium selenolato and tellurolato complexes with the metal in the high formal oxidation state "+5". The reduction of the salicylidene Schiff bases of bis(2-aminophenyl)diselenide and –telluride was performed in situ by released PPh_3 ligands from the oxido- and arylimidorhenium(V) starting materials.[30,31] This methods represents a considerable progress over the hitherto occasionally use of metal(0) species.[32]

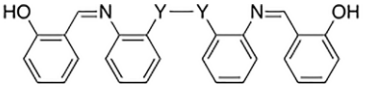

Y = Se: $\{HL^{Se}\}_2$
Y = Te: $\{HL^{Te}\}_2$

In the present work, we demonstrate that the method used for high-valent rhenium complexes can be extended to the metals nickel, palladium and platinum. Thereto, we performed reactions of $[M^{II}Cl_2(PPh_3)_2]$ (M = Ni, Pt) and $[Pd^{II}(OAc)_2(PPh_3)_2]$ with the Schiff bases prepared from salicylaldehyde and bis-(2-aminophenyl)diselenide ($\{HL^{Se}\}_2$) and -ditelluride ($\{HL^{Te}\}_2$).

[a] M. Roca Jungfer, Prof. Dr. U. Abram
Institute of Chemistry and Biochemistry, Freie Universität Berlin,
Fabeckstr. 34/36, 14195 Berlin, Germany
E-mail: Ulrich.Abram@fu-berlin.de
https://www.bcp.fu-berlin.de/chemie/chemie/forschung/InorgChem/agabram/index.html
[b] Prof. Dr. E. S. Lang
Universidade Federal de Santa Maria,
Laboratorio de Materiais Inorganicos, Santa Maria/RS, Brazil
https://www.ufsm.br/cursos/pos-graduacao/santa-maria/ppgq/

Supporting information and ORCID(s) from the author(s) for this article are available on the WWW under https://doi.org/10.1002/ejic.202000750.

Full Paper
doi.org/10.1002/ejic.202000750

Results and Discussion

Reactions of the two dichalcogenide Schiff bases with $[NiCl_2(PPh_3)_2]$, $[PtCl_2(PPh_3)_2]$ or $[Pd(OAc)_2(PPh_3)_2]$ show that they are reduced and form tridentate selenolato and tellurolato ligands. A summary of the performed reactions and obtained products is shown in Scheme 1. The red-orange or red-brown complexes are stable as solids and in solution. Even their solutions can be heated in the air without considerable decomposition. At room temperature, no decomposition or dichalcogenide formation is noticeable even after several days in non-degassed, wet solutions of chlorinated solvents. This is in contrast to the instability of rhenium(V) complexes with the same ligands we reported earlier.[30] Similarly to the reported rhenium complexes, the ^{77}Se signals of the selenolato ligands appear between 197 and 326 ppm and the corresponding ^{125}Te resonances are found between 300 and 477 ppm. The shielding of the chalcogen atoms decreases in the order Pd > Ni > Pt, which has been observed in Schiff base selenolato complexes before.[23] Unfortunately, we could not correlate this shielding trend in the chalcogen chemical shift with any common rationale such as the electronegativity of the involved elements or the solid state geometry of the complexes. The selenium-phosphorus coupling constants are in the range of 21 to 77 Hz. This is within the range of couplings, which have previously been observed for mixed selenolato/phosphine complexes of platinum.[33,34] The ^{125}Te NMR spectra of the analogous tellurolato complexes show doublets with $^2J_{Te,P}$ couplings of 58–194 Hz, which is also in accordance with the situation in previously reported Pt(II) compounds.[33] Unexpectedly, the chalcogen-phosphorus couplings in the nickel complexes are between 77 Hz and 194 Hz, which is four times larger than those of the platinum and palladium complexes. When observed, the ^{77}Se and ^{125}Te couplings in the respective ^{31}P NMR spectra confirm the coupling constants in the ^{77}Se and ^{125}Te spectra. A key feature in the proton NMR spectra of Schiff base complexes is the resonance of their unique aldiminic proton. It is well-separated from the remaining aromatic resonances. As we reported for the rhenium complexes of these ligands, the aldiminic protons in the selenolato complexes are more deshielded compared to those in the tellurolato complexes. The chemical shift of the sulfur analogous nickel complex $[Ni^{II}(L^S)(PPh_3)]$[12] follows the same trend: the aldiminic proton of this compound is more deshielded than that of the selenolato complex $[Ni^{II}(L^{Se})(PPh_3)]$. Additionally, the aldiminic protons are more deshielded along the series nickel-palladium-platinum. In complexes with aldiminic and phosphine ligands, the aldiminic protons often couple to the ^{31}P nuclei. This is also the case in the complexes of the present study with coupling constants in the range of 9–15 Hz. This allows an in situ monitoring of the complex formation. The coupling constants of the selenolato complexes are larger than those of the tellurolato complexes. The platinum NMR resonances of the platinum complexes are observed around –3700 ppm with a $^1J_{Pt,P}$ coupling of ca. 3700 Hz. The $^1J_{Pt,P}$ coupling constants are in the expected range for a phosphine in *trans*-position to a stronger σ-donor with weaker π-accepting abilities.[35] The resonance of $[Pt^{II}(L^{Se})(PPh_3)]$ is more shielded than that of $[Pt^{II}(L^{Te})(PPh_3)]$ and shows a larger coupling to the phosphorus.

Single crystal structure determinations show that the six metal complexes of this study have the same general structure with square-planar coordination spheres of the metal ions bound to tridentate chalcogenolato ligands. The molecular structures of $[Ni(L^{Te})(PPh_3)]$, $[Pd(L^{Te})(PPh_3)]$ and $[Pt(L^{Se})(PPh_3)]$ are shown in Figure 1 as representatives for the complexes with the selenium- and tellurium-containing ligands. Since the general bonding features of the other complexes are similar, their structures are not shown here. They can be found in the Supporting Information. Selected bond lengths and angles of all complexes and the corresponding dichalcogenides[30] are compared in Table 1.

Main distortions of the square-planar coordination environments of the transition metal ions come from the restrictions caused by the size of the chalcogen atoms, the size of the metal ions and the rigidity of the C17–N1 bonds. The two *trans*-spanning angles N1–M1–P1 and O1–M1–Se1/Te1 range from 174.8° to 176.5° and from 172.2° to 179.5° respectively. The N1–M1–Se1/Te1 angles are between 86.8° and 91.0°, while the N1–M1–O1 angles are between 93.3° and 96.8°. The *cis* Se1/Te1–M1–P1 angles are between 91.2° and 96.6°.

In general, the bonding features of the selenium- and tellurium-containing complexes are very similar to the corresponding compounds with the analogous sulfur-containing ligand $\{L^S\}^{2-}$, while the respective complexes with a second phenolato unit, $\{L^O\}^{2-}$, behave differently.[7,9,10,12,15]

The structurally similar complexes of the ligands L^S, L^{Se} and L^{Te} all crystallize in two similar triclinic unit cells. The packing

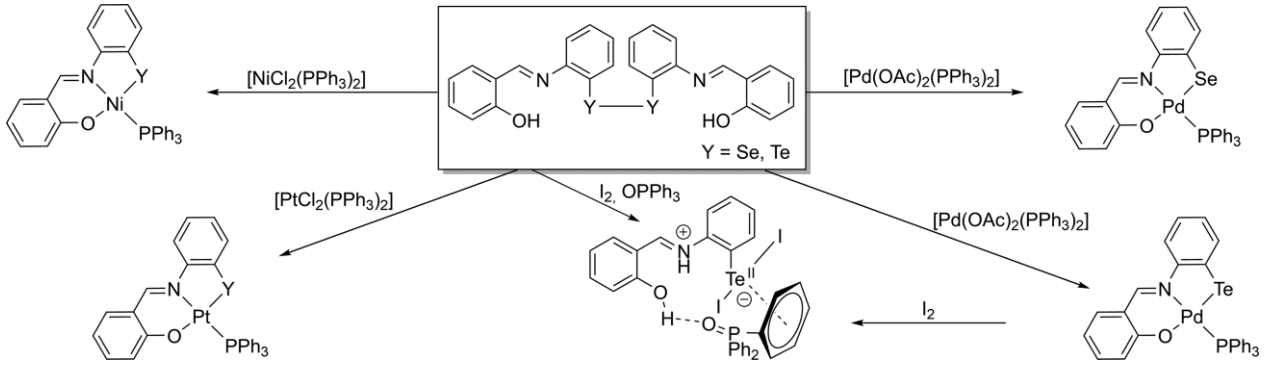

Scheme 1. Performed reactions and their products.

Full Paper
doi.org/10.1002/ejic.202000750

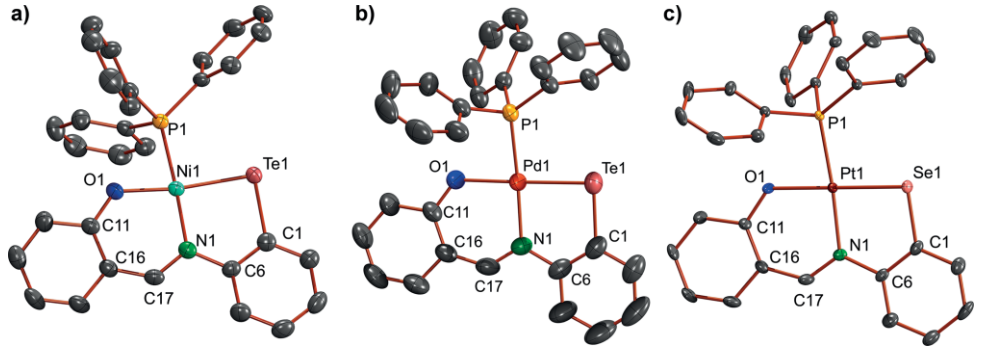

Figure 1. Molecular structures of a) [Ni(L^{Te})(PPh_3)], b) [Pd(L^{Te})(PPh_3)] and c) [Pt(L^{Se})(PPh_3)]. Ellipsoids are depicted at 50 % probability. Hydrogen atoms are omitted for clarity.

Table 1. Selected bond lengths [Å] and angles (°) in the dichalcogenides $\{HL^Y\}_2$[30] and their nickel, palladium and platinum complexes [M(L^Y)(PPh_3)] (Y = Se, Te).

	$\{HL^{Se}\}_2$	[Ni(L^{Se})(PPh_3)]	[Pd(L^{Se})(PPh_3)]	[Pt(L^{Se})(PPh_3)]	$\{HL^{Te}\}_2$	[Ni(L^{Te})(PPh_3)]	[Pd(L^{Te})(PPh_3)]	[Pt(L^{Te})(PPh_3)]
Y1–C1	1.929(2)/1.933(2)	1.900(1)	1.904(3)	1.896(4)	2.127(2)	2.096(3)	2.099(3)	2.11(1)
O1–C11	1.356(2)/1.349(2)	1.303(2)	1.288(3)	1.314(4)	1.356(3)	1.304(4)	1.292(3)	1.31(1)
N1–C6	1.415(2)/1.415(2)	1.438(2)	1.433(3)	1.435(4)	1.415(3)	1.448(4)	1.440(3)	1.40(2)
N1–C17	1.287(2)/1.283(2)	1.310(2)	1.292(3)	1.303(5)	1.287(3)	1.312(4)	1.289(3)	1.28(2)
M1–N1	–	1.915(1)	2.056(2)	2.061(3)	–	1.865(2)	2.041(2)	2.022(8)
M1–O1	–	1.856(1)	2.031(2)	2.031(2)	–	1.933(3)	2.073(2)	2.07(1)
M1–P1	–	2.1900(4)	2.2636(6)	2.2464(9)	–	2.1874(9)	2.2588(6)	2.238(3)
M1–Y1	–	2.2440(3)	2.3402(3)	2.3526(4)	–	2.4050(5)	2.4825(2)	2.502(1)
O1–M1–N1	–	96.46(5)	93.35(7)	93.3(1)	–	96.8(1)	93.29(8)	94.2(4)
O1–M1–P1	–	80.75(3)	84.13(5)	83.34(7)	–	81.01(8)	84.50(5)	81.9(3)
O1–M1–Y1	–	172.88(3)	179.14(7)	179.48(9)	–	172.18(7)	178.85(5)	177.7(2)
N1–M1–P1	–	174.79(4)	176.49(6)	175.71(9)	–	175.01(9)	176.22(6)	174.8(4)
N1–M1–Y1	–	90.63(4)	87.20(5)	86.75(8)	–	91.02(8)	87.82(6)	88.1(3)
Y1–M1–P1	–	92.14(1)	95.35(2)	96.63(2)	–	91.18(3)	94.40(2)	95.85(9)
C1–Y1–M1	–	94.35(4)	95.09(8)	95.3(1)	–	89.48(9)	90.66(8)	89.9(4)

of the [Ni(L^{Se})(PPh_3)], [Ni(L^{Te})(PPh_3)] and [Pt(L^{Te})(PPh_3)] in their unit cells is more compact than that of the other complexes. For most of the structural parameters, a linear dependence with the size of the chalcogen or the size of the metal is observed along the series [M(L^S)(PPh_3)] – [M(L^{Se})(PPh_3)] – [M(L^{Te})(PPh_3)]. The Pd1–Te1 and Pt1–Te1 bonds of 2.4825(2) and 2.502(1) Å are similar to the shortest bond lengths reported in previous studies of palladium[21,25–29,34,36–38] and platinum[39–52] phenyltellurolato complexes. Remarkably and probably as a result of the strain in the five-membered Te1–Ni1–N1 chelate ring, the Ni1–Te1 bond length in [Ni(L^{Te})(PPh_3)] is only 2.4050(5) Å. Compared to the nickel-tellurium bond lengths in the five to date structurally characterized aryltellurolato complexes of nickel, which vary between 2.45 and 2.51 Å, this is surprisingly short. The Ni–Te bonds in [Ni(TePh)Cp(PPh_3)],[53] Ni(TeMes)Cp(PEt_3),[54] [W(CO)$_5$-μ-(TePh)NiCp(PPh_3)][55] and [W(CO)$_4$-μ-{(TePh)NiCp-(PPh_3)}$_2$][55] are relatively long with 2.48 to 2.51 Å, while the shortest known Ni-aryltellurolato bond length reported to date was found in [Ni(NH-C_6H_4-Te)$_2$][56] with 2.4441(6) Å. Of all ca. 40 structurally characterized compounds with a Ni–Te bond, [Ni(NH-C_6H_4-Te)$_2$] as well as [(NiCp*i*Pr^4)$_2$-μ$_2$-(Te$_2$)] (2.440(2) Å),[57] [(NiCp*i*Pr^4)$_2$-μ-(Te)$_2$] (2.44–2.45 Å),[58] [CpFe(C_5H_4)-Te(I)$_2$-Ni(NHC)Cp] (2.4407(8) Å)[59] and (μ$_4$-telluro)-hexakis(μ$_3$-telluro)-bis(μ$_2$-bis(diphenylphosphino)methane)-bis(η$_5$-*tert*-butylcyclopentadienyl)-pentanickeldiniobium (2.436(5) Å)[60] show the overall shortest Ni–Te bond lengths. The Ni–Te bond in [Ni(L^{Te})(PPh_3)] is therefore not only the shortest so far crystallographically determined Ni–Te bond length for an aryltellurolato ligand, but also the shortest Ni–Te distance observed in any compound with a Ni–Te bond.

A more detailed structural comparison of the (almost) full series of [M(L^Y)(PPh_3)] complexes (M = Ni, Pd, Pt; Y = O, S, Se Te) can be found in the Supporting information.

ESI$^+$ mass spectra of the complexes under study clearly show the signals of their molecular ions [M]$^+$ or [M + H]$^+$ ions. In many of the spectra also high-intensity peaks for adducts of the type [2M + cation]$^+$ or ions, which contain protonated, oxidized ligands and reduced metals such as [(MH)$_2$ + H]$^+$, are observed. Additional signals for ions of the composition [M + L^Y + H]$^+$ with an intact, deprotonated dichalcogenide coordinating to one or two metal ions can also be observed. The formation of adducts, the oxidation of the ligands to the dichalcogenides and the reduction of the metal ions occurs mainly for the tellurolato complexes. The presence of such species in the ESI$^+$ mass spectra indicates that compounds such as [M^{II}{L^Y}$_2$], [M^{II}$_2$(L^Y)$_2$] and [M^0$_2${HL^Y}$_2$] with reformed dichalcogenides can formed from [M^{II}(L^Y)(PPh_3)]. In some of the complexes, a fragment of the phosphonium-species {$Ph_3PSe(C_6H_4)$-2-N=CHC_6H_4-2-OH}$^+$ (*m*/*z* = 538.0818) can be observed. This is not unexpected, since such species are also present in the fragmentation patterns of the rhenium complexes, we have studied recently.[30]

The yields reported in the Experimental Section are in the range between 55 and 80 per cent and refer to the isolated pure compounds. But it should be mentioned that the reaction

conditions had to be optimized for parameters such as solvent, temperature and reaction time for each individual complex. This is in analogy to the syntheses of the rhenium(V) complexes with the same ligands,[30] and is explained by a number of relevant, competing side-reactions. Thus, the availability of the precursor molecules in the solution, the release of PPh_3, its favored oxidation to $OPPh_3$ instead of taking part in undesired side-reactions etc. must be controlled carefully. An illustrative example of the requirement for an individual optimization is the reaction of $[Ni^{II}Cl_2(PPh_3)_2]$ with $\{HL^{Se}\}_2$. This reaction generally works at room and elevated temperatures and without the addition of a supporting base in CH_2Cl_2, where it is well soluble. However, under these conditions it is slow and gives unsatisfactorily low yields of $[Ni^{II}(L^{Se})(PPh_3)]$ (ca. 15 %). With regard to our earlier observations, that the yield of such reactions is frequently low when the starting materials are highly soluble in the solvent used for the reaction, we changed the solvent and used boiling acetonitrile, in which the starting materials are insoluble. Upon the addition of a small amount of CH_2Cl_2 to this mixture, a gradual dissolution of the starting materials was observed and the deposition of microcrystalline $[Ni^{II}(L^{Se})(PPh_3)]$ proceeded within minutes with yields of 80 %.

Generally, we found that the presence of traces of water and the absence of oxygen are necessary for good yields. This observation is consistent with the mechanism for the dichalcogenide reduction we proposed for the formation of the related rhenium(V) complexes.[30] Therefore, we believe the mechanism is generally applicable to the reaction of transition metal phosphine complexes with dichalcogenides as is shown in Scheme 2.

Interestingly, an exception to the strict necessity of water are the reactions of $[Pd^{II}(OAc)_2(PPh_3)_2]$ with $\{HL^{Y}\}_2$ (Y = Se, Te), which work slowly at room temperature and without the addition of a supporting base in dry, degassed solvents (yield of $[Pd^{II}(L^{Y})(PPh_3)]$ ca. 50 %). However, also the yield of $[Pd^{II}(L^{Y})(PPh_3)]$ increased to the range of 80 % by the addition of water to the reaction mixture.

To give some rational explanations for the mechanism of the reduction of $\{HL^{Se}\}_2$ with PPh_3 and to the point that it does not proceed without the presence of metal ions,[30] we performed a series of DFT calculations on the B3LYP level for the reactions of free $\{HL^{Se}\}_2$ and metal-bound $\{HL^{Se}\}_2$, in the form of $[Pd\{L^{Se}–HL^{Se}\}(PPh_3)]^+(OAc)^-$, with PPh_3 and H_2O in CH_2Cl_2 solution. Both, a di(organoseleno)phosphorane and an organoselenophosphonium-organoselenolate ion pair were considered as possible intermediates in these reactions. However, the phosphorane intermediates, which were stable intermediates in the gas-phase, did not converge with the solvation model. Therefore, we assume that the ion-pair structures resemble the intermediates in solution better. The summed relative free energies of the respective starting materials, products and intermediates are shown in Scheme 3. Apparently, the release of the phosphonium species is favored for the metal-bound reaction, while it is energetically disfavored for the reaction of free $\{HL^{Se}\}_2$. This is probably due to the stabilization of the complementarily released $\{HL^{Se}\}^-$ anion by the coordination to the metal ion. Furthermore, the energy surface in the metal-bound reaction is much smoother, resulting in better accessible reaction intermediates compared to the reaction of the non-coordinated dichalcogenide.

To get further information about such reactions and possible reasons for the increased reactivity upon coordination, we performed gas-phase calculations on a series of diaryldiselenides R-Se-Se-R (R = Ph, Ph-2-NMe_2, Ph-2-$NCMe_2$, 2-Py, 3-Py-2-NMe_2, 3-Py-2-$NCMe_2$) and their Pd(II) complexes $[PdCl_2(PR'_3)$-η^1-{R-Se-Se-R}] (R'= Ph, Me, CF_3), where we also considered the respective chelated $[PdCl(PR'_3)$-η^2-{R-Se-Se-R}$]^+$ cations. Generally, we found an increase in the intensity and/or size of the σ-hole of the Se-Se bond upon coordination to the metal. This results in an increased polarization of the Se-Se bond and a positive partial charge on the exposed surface of the non-coordinating selenium atom, which bears the majority of the σ*(Se-Se) or σ-hole. For all regarded examples, we then additionally calculated interactions with PPh_3. PPh_3 acts in all (sterically accessible) cases on the metal-bound diselenides as a donor into the σ*(Se-Se) orbitals at the non-coordinated selenium atoms with formation of $[PdCl_2(PR'_3)$-η^1-{R-Se-Se(R)←:PPh_3}]-type donor-acceptor complexes (R'=Me). They show elongated Se-Se bonds (delocalization energy in second order perturbation analysis: 20–60 kcal/mol). In some cases, an inversion of the bonding situation is observed, where the Se-Se bond is broken and a Se–P bond is formed. The resulting selenylphosphonium ions are stabilized in many cases by donation of the liberated selenolato ligands into the σ*-Se-P orbitals: $[PdCl_2(PR'_3)$-η^1-R-

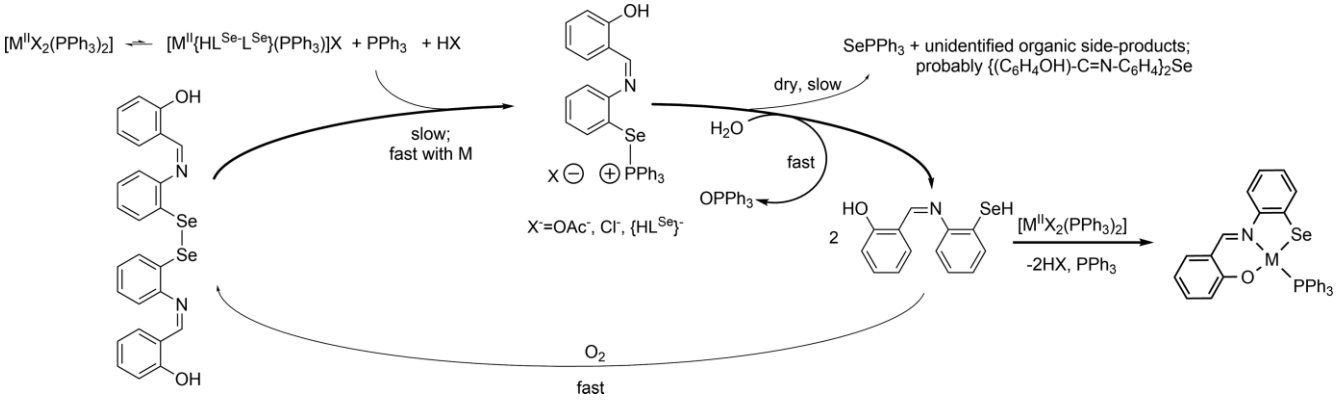

Scheme 2. Proposed mechanism for the reaction between $[MX_2(PPh_3)_2]$ (M = Ni,Pd,Pt) with $\{HL^{Se}\}_2$.

Full Paper
doi.org/10.1002/ejic.202000750

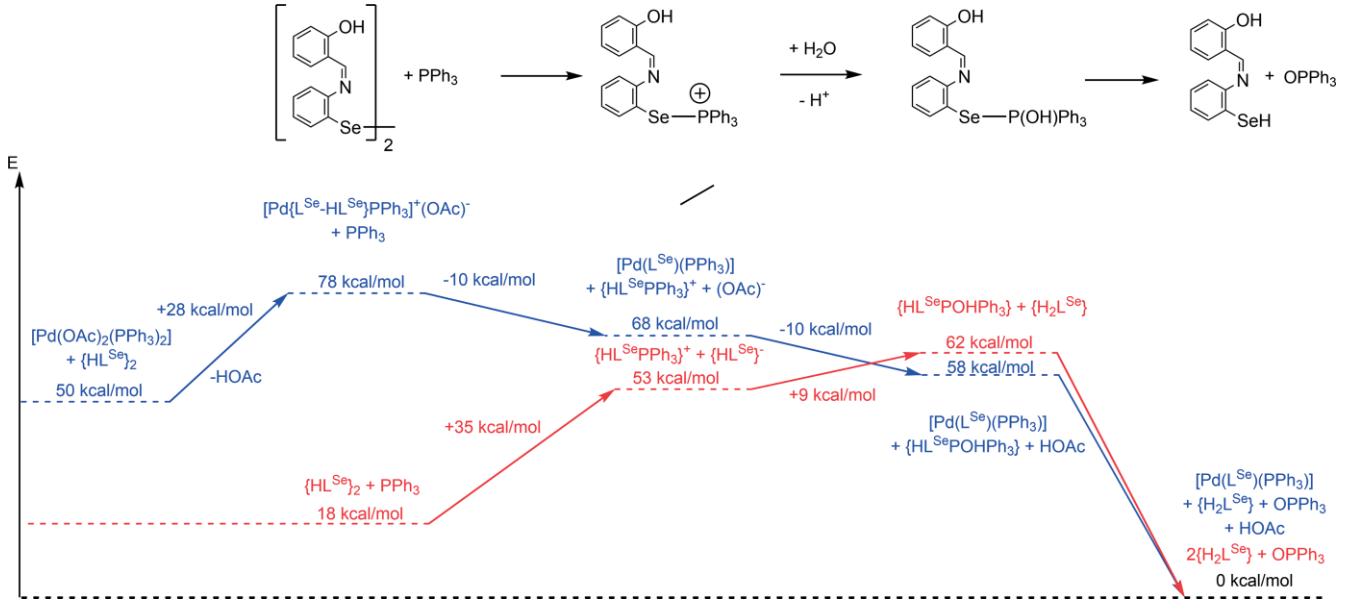

Scheme 3. Differences in free energy between starting materials, products and intermediates suggested for the reaction between free (red) and metal-bound (blue) $\{HL^{Se}\}_2$ with PPh_3 in the presence of water in CH_2Cl_2 solution. The energy values were corrected by the quasi-harmonic method of Grimme.

Se:→Se(R)PPh_3] (R′=Me). The likely reason for the metal-induced reduction is therefore not only the stabilization of the released selenolato anion, but also an increased polarization of the Se-Se bond upon coordination. A positive charge on the metal-diselenide complex further polarizes the non-coordinated selenium atom positively and leads to an even stronger interaction with the phosphine. This commonly results in a cleavage of the Se-Se bond.

In contrast, the donation of PPh_3 to the uncoordinated diselenides is very weak – no formation of donor-acceptor complexes could be concluded and no break of a Se-Se bond is found (maximum delocalization energy in second order perturbation analysis: 2 kcal/mol).

The electrostatic potential maps of the phenyl diselenide model with some further electronic information are shown in Figure 2. Further information on the calculations can be found in the Supporting Information.

Attempted oxidations of the metal(II) complexes with elemental iodine did not result in the formation of defined metal(IV) complexes, but gave intractable, poorly soluble products. Only from the reaction between $[Pd^{II}(L^{Te})(PPh_3)]$ and I_2, which also yields an insoluble dark red powder with low carbon content, a small amount (approximately 10 %) of a crystalline product could be isolated from the remaining solution. It is the zwitterionic compound $[(HO)C_6H_4\text{-}(CHN^+H)\text{-}C_6H_4\text{-}Te^{II}I_2]$, which is associated with one molecule $OPPh_3$ giving a dark purple solid. The same products can be prepared by a direct reaction between $\{L^{Te}\}_2$, I_2 and $OPPh_3$ with somewhat higher yields.

The formation of zwitterionic compounds upon oxidation of diarylditellurides by I_2 is not without precedent and has been observed before e.g. during the reaction of bis(pyridyl)ditelluride with iodine.[61] The stabilization of such zwitterions by long-range interactions with other building blocks is frequently observed and has extensively been studied in a recent work

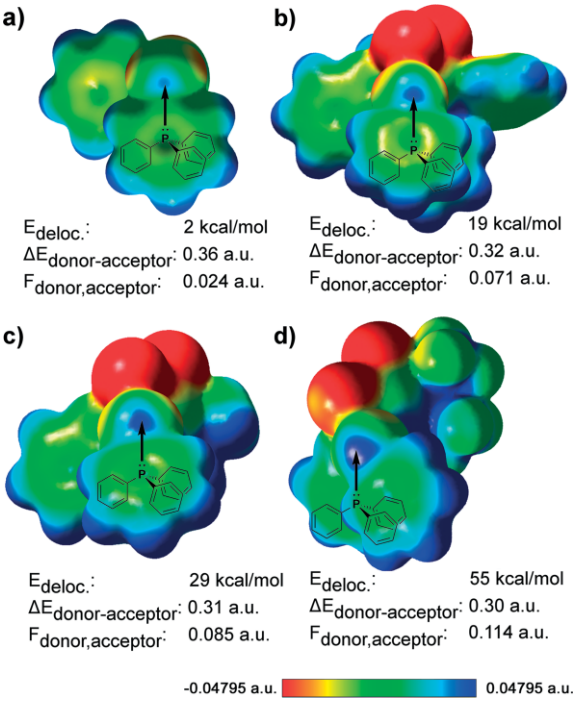

Figure 2. 3D Electrostatic potential maps at the ρ = 0.004 level of the gas-phase calculated model compounds a) $(PhSe)_2$, b) $[PdCl_2(PhSe)_2(PPh_3)]$, c) $[PdCl_2(PhSe)_2(PMe_3)]$ and d) $[PdCl_2(PhSe)_2(P(CF_3)_3)]$. Orientation along the Se-Se bonds with the non-metal-bonded selenium atom and its σ-hole pointing towards the viewer (blue = positive; red = negative; color normalized to the potential of free $(PhSe)_2$). Donation of the PPh_3 lone-pair to the σ-hole on the Se-Se axis centered at the non-coordinating selenium atom is indicated. The estimated second order perturbation energy gain from the donation ($E_{deloc.}$), the energy difference between donor and acceptor orbitals ($\Delta E_{donor-acceptor}$) and the overlap factor ($F_{donor,acceptor}$) are given besides the graphs.

Full Paper
doi.org/10.1002/ejic.202000750

dealing with pyridyltellurium(II) chlorides, bromides and iodides.[62] Long-range interactions play also a role in the solid-state structure of {[(HO)C_6H_4-(CHN$^+$H)-C_6H_4-TeI_2]•$OPPh_3$}. The structure of the compound is shown in Figure 3 and selected bond lengths and angles are summarized in Table 2. The Te1–I1 and Te2–I2 distances are approximately equal and they are bound linearly. One of the phenyl rings in the triphenylphosphine oxide shows a tellurium-centroid distance of 3.771(1) Å and the corresponding Te–centroid contact aligns linearly with the C-Te axis. The individual C=C•••Te distances are between 3.569(1) Å (C22–C23 centroid) and 4.306(1) Å (C25–C26 centroid) and do not align with the C-Te axis. Therefore, it cannot be finally concluded if the observed long range interaction should be attributed to individual C=C•••Te interactions, Ph•••Te interactions or a mixture of both. The infrared spectrum of the zwitterion confirms the protonation of the aldiminic nitrogen atom. A sharp N-H stretch of medium intensity is observed at 3050 cm^{-1}. The intense band for the O-H stretch is very broad and centered at 2324 cm^{-1}. The ESI$^+$ mass spectrum of {[(HO)C_6H_4-(CHN$^+$H)-C_6H_4-TeI_2]•$OPPh_3$} is less instructive and mainly contains peaks, which are related to triphenylphosphine oxide.

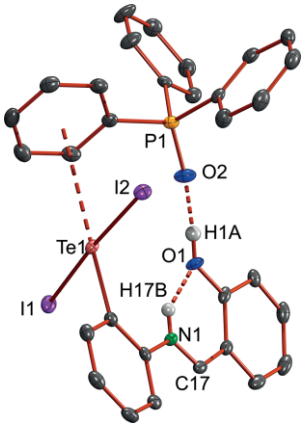

Figure 3. Structure of {[(HO)C_6H_4-(CHN$^+$H)-C_6H_4-TeI_2]•$OPPh_3$}. Ellipsoids are depicted at 50 % probability. Hydrogen atoms bonded to carbon atoms are omitted for clarity.

Table 2. Selected bond lengths [Å] and angles (°) in {[(HO)C_6H_4-(CHN$^+$H)-C_6H_4-$Te^{II}I_2$]•$OPPh_3$}.

Te1–I1	2.9466(9)	N1–C17	1.303(4)	
Te1–I2	2.969(1)	P1–O2	1.497(2)	
Te–Centroid	3.771(1)			
C-Te1–I1	88.36(8)	C-Te1–I2	89.90(8)	
I1–Te1–I2	176.181(9)	C-Te–centroid	179.32(8)	
I1–Te1-centroid	91.84(1)	I2–Te1-centroid	89.86(1)	
D–H•••A	d(D–H)	d(H•••A)	d(D•••A)	<(DHA)
N1–H17B•••O1	0.80(3)	1.95(3)	2.604(3)	138(3)
O1–H1•••O2	0.81(4)	1.70(4)	2.506(3)	171(4)

Conclusions

In the present communication, we extended the recently reported method, in which released PPh_3 acts as reducing agent for metal-bound dichalcogenides to nickel, palladium and platinum. All three group 10 elements form stable complexes with the tridentate selenolato- and tellurolato-substituted Schiff base ligands {HL^{Se}}$^{2-}$ and {HL^{Te}}$^{2-}$, respectively. The resulting [M(L^Y)(PPh_3)] complexes (Y = Se, Te) have a square-planar coordination geometry. Optimum yields are obtained in the presence of water and under strict exclusion of dioxygen. The intermediates of the reactions of [$Pd(OAc)_2(PPh_3)_2$] and {HL^{Se}}$_2$ as well as {HL^{Se}}$_2$ with PPh_3 were evaluated via DFT calculations. Calculations about the coordination of several model diselenides to a palladium(II) center reveal an increased polarization of the Se-Se bonds upon coordination, which facilitates the nucleophilic attack of PPh_3. The stabilization of the {L^{Se}}$^{2-}$ anion by coordination to a metal ion results in the stabilization of an intermediate {L^{Se}-PPh_3}$^+$ phosphonium salt, which is less stable without the presence of a metal. Therefore, the reduction does not (or only very slowly) proceed without the presence of metal ions.

Experimental Section

[$NiCl_2(PPh_3)_2$],[63] [$Pd(OAc)_2$],[64] [$Pd(OAc)_2(PPh_3)_2$],[64] [$PtCl_2(PPh_3)_2$],[65–67] {HL^{Se}}$_2$,[30] {HL^{Te}}$_2$,[30] bis(2-aminophenyl) diselenide and bis-(2-aminophenyl)ditelluride were prepared according to literature procedures.[68–70] All other chemicals were reagent grade and used as received. Reactions involving oxygen- or water-sensitive compounds were performed with standard Schlenk technique. Large amounts of solvents were degassed using three freeze-pump-thaw cycles with Ar as the filling gas. Small amounts of solvents were alternatively degassed by bubbling a strong stream of argon through the solvent for 15–30 min immediately before use.

NMR spectra were recorded at 25 °C on JEOL 400 MHz ECS-400 or JNM-ECA400II spectrometers. Reported chemical shifts (δ) are referenced according to the IUPAC recommendations of 2008.[71] External reference standards: tetramethylsilane, (^{1}H, ^{13}C), $ClCF_3$ (^{19}F), 85 % phosphoric acid (^{31}P), dimethylselenide (^{77}Se), dimethyltelluride (^{125}Te) and 1.2 M $Na_2[PtCl_4]$ in D_2O (^{195}Pt).

IR-Spectra were recorded with an FT IR spectrometer (Nicolet iS10, Thermo Scientific). Intensities are classified as vs. = very strong, s = strong, m = medium, w = weak, vw = very weak, sh = shoulder.

Electrospray ionization mass spectrometry (ESI MS) was carried out with the ESI MSD TOF unit of an Agilent 6210 TOF LC/MS system. The measurements were performed in $CHCl_3$, CH_2Cl_2, MeOH, DMSO or mixtures of them.

Elemental analyses were performed using a vario EL III CHN elemental analyzer (Elementar Analysensysteme GmbH) or a vario MICRO cube CHNS elemental analyzer. Some of the determined carbon values of the metal complexes show slightly too low contents. This is a systematic finding on our analyzers and might have to do with the formation of carbides.

Single crystal X-ray diffraction data were collected on a Bruker D8 Venture or a STOE IPDS II T. Absorption corrections were carried out by the multiscan (Bruker D8 Venture) or integration methods (STOE IPDS II T).[72,73] Structure solutions and refinements were done with the SHELX-2008, SHELX-2014 and SHELX-2016 program packages.[74,75] Hydrogen atom positions at heteroatoms or the aldiminic carbon atoms were taken from the Fourier maps when possible or placed at calculated positions and refined by a riding model. All other hydrogen atoms were placed at calculated posi-

tions and refined by a riding model. The visualization of the molecular structures was done using the program DIAMOND 4.2.2.[76]

CCDC 2021656 (for [Ni(L^{Se})(PPh_3)]), 2021657 (for [Ni(L^{Te})(PPh_3)]), 2021658 (for [Pd(L^{Se})(PPh_3)]), 2021659 (for [Pd(L^{Te})(PPh_3)]), 2021660 (for [Pt(L^{Se})(PPh_3)]), 2021661(for [Pt(L^{Te})(PPh_3)]) and 2021662 (for {[(HO)C_6H_4-(CHN^+H)-C_6H_4-TeI_2]•$OPPh_3$}) contain the supplementary crystallographic data for this paper. These data can be obtained free of charge from The Cambridge Crystallographic Data Centre.

DFT calculations were performed on the high-performance computing systems of the Freie Universität Berlin ZEDAT (Curta) using the program packages GAUSSIAN 09 and GAUSSIAN 16.[77,78] The gas phase and solution geometry optimizations were performed using coordinates derived from the X-ray crystal structures using GAUSSVIEW.[79] The polarizable continuum model (PCM) with the integral equation formalism variant (IEFPCM) was used to implicitly simulate the solvent dichloromethane. The calculations were performed with the hybrid density functional B3LYP.[80–82] The double-ζ pseudopotential LANL2DZ basis set with the respective effective core potential (ECP) was applied to Ni, Pd and Pt.[83] The Stuttgart relativistic large core basis set RLC with the corresponding ECP was applied to I.[84] The Stuttgart relativistic large core basis set RLC with the corresponding ECP and an extension by STO-3G* polarization functions was applied to Te.[84,85] The 6-31G* basis set was applied for all other atoms excluding H.[86–90] For H, the 6-31G basis set was applied.[91] All basis sets as well as the ECPs were obtained from the EMSL database.[92] Frequency calculations after the optimizations confirmed the convergence. No negative frequencies were obtained for the given optimized geometries of all compounds. The entropic contribution to the free energy was corrected for low-energy modes using the quasi-harmonic approximation of Grimme[93] as implemented in the freely accessible python code *GoodVibes* of Funes-Ardoiz and Paton with a cut-off at 500 cm^{-1}.[94] Further analysis of orbitals, charges, 2D ESP mapping, QTAIM, etc. was performed with the free multifunctional wavefunction analyzer *Multiwfn*.[95] Vizualisation of the electrostatic potential maps was done with GAUSSVIEW.[79] To verify the suitability of the employed methods, the structures of all [M(L^Y)(PPh_3)] (M = Ni, Pd, Pt; Y = O, S, Se, Te) were calculated in the gas-phase. The calculated bonding parameters match the determined crystal structures, where they were available, on average within 0.036 Å. The deviations are highest with an average elongation of 0.054 Å for the coordination sphere of the metals, which is expected for a gas phase calculation. The latter is most prominent in the metal tellurium distances with an average elongation of 0.115 Å compared to the solid-state structures.

[Ni(L^{Se})(PPh_3)]. [$NiCl_2(PPh_3)_2$] (66 mg, 0.1 mmol) and {HL^{Se}}$_2$ (22 mg, 0.04 mmol) were suspended in degassed CH_3CN (6 mL). and heated to reflux. CH_2Cl_2 (1 mL) was added and the color of the suspension changed from dark green to dark brown. After 5 min, the solution was cooled to room temperature. Diethyl ether (24 mL) was added to the yellow solution with a brown precipitate. The mixture was left in the freezer overnight to finish the precipitation. The brown-red microcrystals were filtered off, washed with diethyl ether and dried in vacuo. A second crop of crystals was obtained by evaporation of the combined filtrates and washing solutions. The product can be recrystallized from CH_2Cl_2/diethyl ether or CH_2Cl_2/EtOH. Brown-red microcrystals or red-green dichroic cubes. Yield: 36 mg (76 %).

Elemental analysis: Calculated for $C_{31}H_{24}NNiOPSe$: C 62.6, H 4.1, N 2.4 %; Found C 62.0, H 4.1, N 2.3 %. IR (cm^{-1}): $\tilde{\nu}$ = 3058 (w), 1605 (m) C=N, 1580 (m), 1564 (m), 1523 (m), 1478 (m), 1455 (m), 1431 (s), 1377 (m), 1366 (m), 1332 (m), 1307 (w), 1262 (m), 1248 (m), 1225 (m), 1169 (m), 1157 (m), 1145 (m), 1123 (m), 1100 (sh), 1092 (s), 1038 (m), 1025 (m), 997 (m), 976 (vw), 950 (w), 926 (m), 841 (m), 806 (m), 756 (sh), 744 (vs), 715 (sh), 702 (sh), 690 (vs), 618 (w), 609 (m), 555 (s), 548 (m). ESI^+ MS (*m/z*): 538.0856 (calc. 538.0843) [HL^{Se} + PPh_3]$^+$, 596.0193 (calc. 596.0191) [M + H]$^+$, 618.0017 (calc. 618.0010) [M + Na]$^+$, 633.9753 (calc. 633.9750) [M + K]$^+$. ^{1}H NMR (CD_2Cl_2, ppm): 8.86 (1H, d, $^4J_{H,P}$ = 9.29 Hz, **H17**CR=NR), 7.96–7.79 (6H, m, *m*-P-Ar**H**), 7.62 (1H, d, $^3J_{H15,H14}$ = 8.31 Hz, ^{L}Ar**H15**), 7.56–7.48 (3H, m, *p*-P-Ar**H**), 7.56–7.48 (8H, m, 6 *o*-P-Ar**H**, ^{L}Ar**H2** [ca. 7.44], ^{L}Ar**H12** [ca. 7.41]), 7.17 (1H, m, ^{L}Ar**H4**), 7.09 (1H, m, ^{L}Ar**H14**), 6.98 (1H, m, ^{L}Ar**H13**), 6.64 (1H, m, ^{L}Ar**H3**), 6.33 (1H, d, $^3J_{H5,H4}$ = 8.31 Hz, ^{L}Ar**H5**). ^{13}C NMR (CD_2Cl_2, ppm): 164.4 (d, $^3J_{C,P}$ = 1 Hz, ^{L}**C$_{Ar}$6**), 157.1 (s, H**C17**R=NR), 152.5 (d, $^3J_{C,P}$ = 10 Hz, ^{L}**C$_{Ar}$11**), 135.7 (d, $^4J_{C,P}$ = 14 Hz, ^{L}**C$_{Ar}$16**), 134.9 (d, $^3J_{C,P}$ = 10 Hz, *m*-P-**C$_{Ar}$**), 134.7 (s, ^{L}**C$_{Ar}$2**), 134.6 (s, ^{L}**C$_{Ar}$4**), 130.9 (d, $^4J_{C,P}$ = 3 Hz, *p*-P-**C$_{Ar}$**), 130.6 (d, $^3J_{C,P}$ = 2 Hz, ^{L}**C$_{Ar}$1**-Se), 129.8 (d, $^1J_{C,P}$ = 46 Hz, P-**C$_{Ar}$**), 128.4 (d, $^2J_{C,P}$ = 10 Hz, *o*-P-**C$_{Ar}$**), 127.0 (s, ^{L}**C$_{Ar}$13**), 123.5 (s, ^{L}**C$_{Ar}$14**), 121.6 (d, $^4J_{C,P}$ = 1 Hz, ^{L}**C$_{Ar}$5**), 119.8 (s, ^{L}**C$_{Ar}$12**), 116.5 (s, ^{L}**C$_{Ar}$15**), 115.7 (s, ^{L}**C$_{Ar}$3**). ^{31}P NMR (CD_2Cl_2, ppm): 22.1 (s). ^{77}Se NMR (CD_2Cl_2, ppm): 233.0 (d, $^2J_{Se,P}$ = 77 Hz).

[Ni(L^{Te})(PPh_3)]. [$NiCl_2(PPh_3)_2$] (66 mg, 0.1 mmol) and {HL^{Te}}$_2$ (22 mg, 0.08 mmol) were suspended in degassed EtOH (2 mL). and heated to reflux. NEt_3 (3 drops) was added and the mixture was heated under reflux for further 15 min. After cooling to room temperature, the dark precipitate was filtered off and washed with water, diethyl ether and hexane. It was dried in vacuo. A second crop of crystals was obtained by layering the combined filtrate and washing solutions with hexane. Brown-red microcrystals or red-green dichroic cubes. Yield: 40 mg (59 %).

Elemental analysis: Calculated for $C_{31}H_{24}NNiOPTe$: C 57.8, H 3.8, N 2.2 %; Found C 57.5, H 3.8, N 2.1 %. IR (cm^{-1}): $\tilde{\nu}$ = 3060 (w), 1606 (m) C=N, 1581 (m), 1563 (m), 1522 (m), 1479 (m), 1453 (m), 1431 (s), 1381 (m), 1365 (m), 1337 (m), 1259 (m), 1247 (m), 1222 (m), 1169 (m), 1156 (m), 1146 (s), 1126 (m), 1101 (s), 1091 (s), 1044 (w), 1028 (m), 997 (m), 952 (w), 926 (m), 841 (m), 805 (m), 758 (sh), 744 (vs), 715 (sh), 701 (sh), 690 (vs), 618 (w), 604 (m), 555 (s), 546 (m), 528 (s). ESI^+ MS (*m/z*): 706.8907 (calc. 706.8890) [Ni{HL^{Te}}$_2$ + H], 728.8723 (calc. 728.8709) [Ni{HL^{Te}}$_2$ + Na], 744.8459 (calc. 744.8447) [Ni{HL^{Te}}$_2$ + K], 1410.7711 (calc. 1410.7700) [2Ni{HL^{Te}}$_2$ + H], 1432.7522 (calc. 1432.7519) [2Ni{HL^{Te}}$_2$ + Na], 1448.7282 (calc. 1448.7257) [2Ni{HL^{Te}}$_2$ + K], 1526.7746 (calc. 1526.7091) [2Ni{HL^{Te}}$_2$ + Ni(OAc)]. ^{1}H NMR ($CDCl_3$, ppm): 8.47 (1H, d, $^4J_{H,P}$ = 8.23 Hz, **H17**CR=NR), 7.87–7.66 (6H, m, *m*-P-Ar**H**), 7.46 (1H, d, $^3J_{H15,H14}$ = 7.58 Hz, ^{L}Ar**H15**), 7.40–7.09 (11H corrected for $CHCl_3$, m, *p*-P-Ar**H**, *o*-P-Ar**H**, ^{L}Ar**H2**, ^{L}Ar**H12**), 6.99 (2H, m, ^{L}Ar**H4**, ^{L}Ar**H14**), 6.79 (1H, m, ^{L}Ar**H13**), 6.45 (1H, m, ^{L}Ar**H3**), 6.10 (1H, d, $^3J_{H5,H4}$ = 8.58 Hz, ^{L}Ar**H5**). ^{13}C NMR ($CDCl_3$, ppm): 164.8 (s, ^{L}**C$_{Ar}$6**), 159.9 (s, H**C17**R=NR), 158.6 (s, ^{L}**C$_{Ar}$11**), 135.3 (s, ^{L}**C$_{Ar}$2**), 134.8 (s, ^{L}**C$_{Ar}$4**), 134.7 (d, $^3J_{C,P}$ = 6 Hz, *m*-P-**C$_{Ar}$**), 134.7 (overlapped s (in the middle of the d for *m*-P-C_{Ar}), ^{L}**C$_{Ar}$16**), 132.2 (d, $^4J_{C,P}$ = 10 Hz, ^{L}**C$_{Ar}$16**), 130.6 (s, *p*-P-**C$_{Ar}$**), 130.6 (d, $^1J_{C,P}$ = 48 Hz, P-**C$_{Ar}$**), 128.2 (d, $^2J_{C,P}$ = 10 Hz, *o*-P-**C$_{Ar}$**), 126.6 (s, ^{L}**C$_{Ar}$13**), 125.2 (s, ^{L}**C$_{Ar}$14**), 121.9 (s, ^{L}**C$_{Ar}$5**), 120.1 (s, ^{L}**C$_{Ar}$12**), 118.1 (s, ^{L}**C$_{Ar}$15**), 115.3 (s, ^{L}**C$_{Ar}$3**), 112.4 (d, $^3J_{C,P}$ = 11 Hz, ^{L}**C$_{Ar}$1**-Te). ^{31}P NMR ($CDCl_3$, ppm): 25.6 (s), 25.5 (d, $^2J_{P,Te}$ = 191 Hz, P-Ni-^{125}Te). ^{125}Te NMR ($CDCl_3$, ppm): 338.6 (d, $^2J_{Te,P}$ = 194 Hz).

[Pd(L^{Se})(PPh_3)]. [$Pd(OAc)_2(PPh_3)_2$] (112 mg, 0.15 mmol) was dissolved in a degassed mixture of CH_2Cl_2 (3 mL) and water (3 drops). {HL^{Se}}$_2$ (83 mg, 0.15 mmol) was added as a solid. The color of the solution turned from yellow to red immediately and the mixture was stirred vigorously for 3 h. It was layered with diethyl ether (18 mL) and left in the freezer. After 3 days, large red crystals had formed, which were filtered off, washed with diethyl ether and dried in vacuo. A second crop of crystals was obtained by evaporation

of the combined filtrate and washing solutions. Orange-red plates. Yield: 76 mg (78 %).

Elemental analysis: Calculated for $C_{31}H_{24}NOPPdSe$: C 57.9, H 3.8, N 2.1 %; Found C 56.8, H 3.9, N 2.1 %. IR (cm^{-1}): $\tilde{\nu}$ = 3047 (w), 3015 (w), 1967 (w), 1911 (w), 1605 (m) C=N, 1587 (m), 1571 (m), 1522 (m), 1482 (m), 1457 (m), 1433 (s), 1387 (m), 1364 (m), 1332 (m), 1308 (w), 1306 (w), 1263 (w), 1250 (w), 1219 (w), 1191 (m) 1171 (m), 1148 (s), 1125 (m), 1098 (s), 1037 (sh), 1028 (m), 997 (m), 948 (w), 929 (m), 850 (w), 838 (w), 800 (w), 748 (sh), 736 (vs), 709 (sh), 693 (vs), 642 (w), 616 (w), 607 (m), 577 (vw), 565 (w), 551 (s), 531 (s). ESI^+ MS (*m/z*): 643.9895 (calc. 643.9888) $[M + H]^+$, 665.9718 (calc. 665.9707) $[M + Na]^+$, 681.9452 (calc. 681.9446) $[M + K]^+$, 944.0577 (calc. 944.00364) $[M + PPh_3 + K]^+$, 1308.9532 (calc. 1308.9536) $[2M + Na]^+$, 1324.9274 (calc. 1324.9274) $[2M + K]^+$. ^1H NMR (CD_2Cl_2, ppm): 8.94 (1H, d, $^4J_{H,P}$ = 14.98 Hz, **H17**CR=NR), 7.85–7.73 (6H, m, *m*-P-Ar**H**), 7.69 (1H, d, $^3J_{H15,H14}$ = 7.89 Hz, ^{L}Ar**H15**), 7.60–7.41 (11H corrected for $CHCl_3$, m, *p*-P-Ar**H**, *o*-P-Ar**H**, ^{L}Ar**H2** [ca. 7.48], ^{L}Ar**H12** [ca. 7.44]), 7.32 (1H, m, ^{L}Ar**H4**), 7.14 (1H, m, ^{L}Ar**H13**), 7.03 (1H, m, ^{L}Ar**H12**), 6.70–6.62 (2H, m, ^{L}Ar**H3** [ca. 6.64], ^{L}Ar**H5** [ca. 6.62]). ^{13}C NMR (CD_2Cl_2, ppm): 165.6 (s, ^{L}**C$_{Ar}$6**), 156.3 (s, H**C17**R=NR), 151.2 (d, $^3J_{C,P}$ = 2 Hz, ^{L}**C$_{Ar}$11**), 136.6 (s, ^{L}**C$_{Ar}$2**), 135.8 (s, ^{L}**C$_{Ar}$4**), 135.0 (d, $^3J_{C,P}$ = 11 Hz, *m*-P-**C$_{Ar}$**), 134.9 (s, ^{L}**C$_{Ar}$16**), 131.3 (d, $^4J_{C,P}$ = 3 Hz, *p*-P-**C$_{Ar}$**), 131.3 (d, $^3J_{C,P}$ = 1 Hz, ^{L}**C$_{Ar}$1**-Se), 129.8 (d, $^1J_{C,P}$ = 51 Hz, P-**C$_{Ar}$**), 128.5 (d, $^2J_{C,P}$ = 11 Hz, *o*-P-**C$_{Ar}$**), 127.3 (s, ^{L}**C$_{Ar}$13**), 123.8 (s, ^{L}**C$_{Ar}$14**), 122.0 (d, $^4J_{C,P}$ = 2 Hz, ^{L}**C$_{Ar}$5**), 119.7 (s, ^{L}**C$_{Ar}$12**), 116.9 (d, $^5J_{C,P}$ = 1 Hz, ^{L}**C$_{Ar}$15**), 115.1 (s, ^{L}**C$_{Ar}$3**). ^{31}P NMR (CD_2Cl_2, ppm): 25.6 (s). ^{77}Se NMR (CD_2Cl_2, ppm): 326.4 (dd, $^2J_{Se,P}$ = 21 Hz, *J* = 6 Hz).

[Pd(L^{Te})(PPh_3)]. $[Pd(OAc)_2(PPh_3)_2]$ (72 mg, 0.1 mmol) was dissolved in a degassed mixture of CH_2Cl_2 (1 mL) and water (1 drop). $\{HL^{Te}\}_2$ (64 mg, 0.1 mmol) was added as a solid. The color of the solution turned immediately from yellow to brown. The mixture was stirred vigorously for 3 h. It was layered with diethyl ether (18 mL) and left in the freezer overnight. The large deep red crystals, which formed, were filtered off. They were washed with diethyl ether and hexane and dried in vacuo. A second crop of crystals was obtained by evaporation of the combined filtrate and washing solutions. Dark red blocks. Yield: 52 mg (75 %).

Elemental analysis: Calculated for $C_{31}H_{24}NOPPdTe$: C 53.8, H 3.5, N 2.0 %; Found C 53.6, H 3.6, N 2.0 %. IR (cm^{-1}): $\tilde{\nu}$ = 3048 (w), 1605 (m) C=N, 1582 (m), 1566 (sh), 1558 (m), 1518 (m), 1505 (sh), 1480 (m), 1450 (m), 1431 (s), 1390 (m), 1368 (m), 1335 (m), 1308 (w), 1287 (vw), 1259 (m), 1244 (m), 1215 (w), 1182 (m), 1164 (m), 1157 (sh), 1146 (s), 1128 (m), 1102 (s), 1093 (sh), 1069 (w), 1044 (w), 1027 (m), 997 (m), 969 (w), 953 (w), 926 (m), 841 (m), 794 (w), 757 (sh), 743 (vs), 716 (m), 716 (sh), 703 (vs), 637 (vw), 618 (w), 602 (m), 573 (vw), 550 (m), 530 (s). ESI^+ MS (*m/z*): 693.9772 (calc. 693.9771) $[M + H]^+$, 715.9657 (calc. 715.9591) $[M + Na]^+$, 731.9346 (calc. 731.9328) $[M + K]^+$, 944.0577 (calc. 944.00364) $[M + PPh_3 + K]^+$, 1152.8675 (calc. 1152.8998) $[\{Pd^0(PPh_3)(HL^{Te})\text{-}(HL^{Te})Pd^0H_2\} + Na]^+$. ^1H NMR (CD_2Cl_2, ppm): 8.72 (1H, d, $^4J_{H,P}$ = 14.09 Hz, **H17**CR=NR), 7.83–7.72 (6H, m, *m*-P-Ar**H**), 7.46 (1H, dd, $^3J_{H15,H14}$ = 7.64 Hz, $^4J_{H15,H12}$ = 1.32 Hz, ^{L}Ar**H15**), 7.56–7.48 (3H, m, *p*-P-Ar**H**), 7.48–7.39 (8H, m, 6 *o*-P-Ar**H**, ^{L}Ar**H2**, ^{L}Ar**H12**), 7.29 (1H, ddd, $^3J_{H4,H5}$ = 8.64 Hz, $^3J_{H4,H3}$ = 6.78 Hz, $^4J_{H4,H2}$ = 1.88 Hz, ^{L}Ar**H4**), 7.20 (1H, m, ^{L}ArH**14**), 6.96 (1H, m, ^{L}Ar**H13**), 6.61 (1H, ddd, $^3J_{H3,H2}$ = 7.95 Hz, $^3J_{H3,H4}$ = 6.78 Hz, $^4J_{H3,H5}$ = 1.14 Hz, ^{L}Ar**H3**), 6.54 (1H, d, $^3J_{H5,H4}$ = 8.64 Hz, ^{L}Ar**H5**). ^{13}C NMR (CD_2Cl_2, ppm): 166.6 (s, ^{L}**C$_{Ar}$6**), 159.6 (s, H**C17**R=NR), 157.3 (d, $^3J_{C,P}$ = 2 Hz, ^{L}**C$_{Ar}$11**), 137.2 (s, ^{L}**C$_{Ar}$2**), 136.4 (s, ^{L}**C$_{Ar}$4**), 136.1 (d, $^4J_{C,P}$ = 1 Hz, ^{L}**C$_{Ar}$16**), 135.2 (d, $^3J_{C,P}$ = 11 Hz, *m*-P-**C$_{Ar}$**), 131.5 (d, $^4J_{C,P}$ = 3 Hz, *p*-P-**C$_{Ar}$**), 131.0 (d, $^1J_{C,P}$ = 52 Hz, P-**C$_{Ar}$**), 128.8 (d, $^2J_{C,P}$ = 11 Hz, *o*-P-**C$_{Ar}$**), 127.3 (s, ^{L}**C$_{Ar}$13**), 125.7 (s, ^{L}**C$_{Ar}$14**), 122.2 (d, $^4J_{C,P}$ = 2 Hz, ^{L}**C$_{Ar}$5**), 120.1 (s, ^{L}**C$_{Ar}$12**), 118.9 (d, $^5J_{C,P}$ = 1 Hz, ^{L}**C$_{Ar}$15**), 115.1 (s, ^{L}**C$_{Ar}$3**), 112.1 (d, $^3J_{C,P}$ = 6 Hz, ^{L}**C$_{Ar}$1**-Te). ^{31}P NMR (CD_2Cl_2, ppm): 21.7 (s), 21.7 (d, $^2J_{P,Te}$ = 53 Hz, P-Pd-^{125}Te). ^{125}Te NMR (CD_2Cl_2, ppm): 476.5 (d, $^2J_{Te,P}$ = 61 Hz).

[Pt(L^{Se})(PPh_3)]. $[PtCl_2(PPh_3)_2]$ (80 mg, 0.1 mmol) and $\{HL^{Se}\}_2$ (44 mg, 0.08 mmol) were suspended in a degassed mixture of EtOH (1 mL) and CH_2Cl_2 (1 mL). The yellow-beige solution was heated to reflux and NEt_3 (3 drops) was added, which resulted in a color change to orange-red. After 30 min, the mixture was cooled to room temperature, the bright orange precipitate was filtered off and washed with diethyl ether and hexane. It was dried in vacuo. The product can be recrystallized by slow diffusion of diethyl ether into a CH_2Cl_2 solution. Bright orange-red powder or orange-red needles. Yield: 55 mg (75 %).

Elemental analysis: Calculated for $C_{31}H_{24}NOPPtSe$: C 50.9, H 3.3, N 1.9 %; Found C 50.8, H 3.4, N 1.9 %. IR (cm^{-1}): $\tilde{\nu}$ = 3047 (w), 1605 (m) C=N, 1587 (m), 1573 (m), 1524 (m), 1482 (m), 1459 (m), 1434 (s), 1387 (m), 1366 (m), 1329 (m), 1297 (w), 1264 (w), 1250 (w), 1221 (w), 1191 (w), 1172 (m), 1149 (m), 1126 (m), 1099 (s), 1049 (w), 1038 (w), 1028 (m), 996 (w), 960 (vw), 945 (vw), 931 (sh), 921 (w), 867 (w), 850 (w), 837 (w), 804 (w), 749 (sh), 735 (vs), 709 (sh), 694 (vs), 644 (vw), 616 (m), 585 (w), 567 (vw), 556 (m), 538 (vs), 526 (s). ESI^+ MS (*m/z*): 754.0342 (calc. 754.0304) $[M + Na]^+$, 770.0092 (calc. 770.0043) $[M + K]^+$, 1486.0782 (calc. 1486.0738) $[2M + Na]^+$, 1503.0516 (calc. 1503.0476) $[2M + K]^+$. ^1H NMR ($CDCl_3$, ppm): 9.20 (1H, d, $^4J_{H,P}$ = 13.29 Hz, **H17**CR=NR), 9.20 (dd, $^3J_{H,Pt}$ = 42.98 Hz, $^4J_{H,P}$ = 11.08 Hz, **H17**CR=NR), 9.20 (dd, $^1J_{C17,H17}$ = 161.48 Hz, $^4J_{H,P}$ = 12.69 Hz, **H17**CR=NR), 7.85–7.75 (6H, m, *m*-P-Ar**H**), 7.70 (1H, dd, $^3J_{H15,H14}$ = 7.72 Hz, $^4J_{H15,H13}$ = 1.48 Hz, ^{L}Ar**H15**), 7.57 (1H, dd, $^3J_{H12,H13}$ = 8.01 Hz, $^4J_{H12,H14}$ = 1.83 Hz, ^{L}Ar**H12**), 7.53–7.38 (11H, m, *p*-P-Ar**H**, *o*-P-Ar**H**, ^{L}Ar**H2**, ^{L}Ar**H14**), 7.09 (1H, ddd, $^3J_{H13,H12}$ = 8.38 Hz, $^4J_{H13,H14}$ = 6.81 Hz, $^4J_{H13,H15}$ = 1.53 Hz, ^{L}Ar**H13**), 7.02 (1H, ddd, $^3J_{H4,H3}$ = 8.08 Hz, $^4J_{H4,H5}$ = 7.04 Hz, $^4J_{H4,H2}$ = 1.18 Hz, ^{L}Ar**H4**), 6.75–6.90 (2H, m + ddd, $^3J_{H3,H4}$ = 7.93 Hz, $^3J_{H3,H2}$ = 6.77 Hz, $^3J_{H3,H5}$ = 1.15 Hz, ^{L}Ar**H5**, ^{L}Ar**H3**). ^{13}C NMR ($CDCl_3$, ppm): 163.1 (s, ^{L}**C$_{Ar}$6**), 153.3 (s, H**C17**R=NR), 150.8 (d, $^3J_{C,P}$ = 1 Hz, ^{L}**C$_{Ar}$11**), 135.3 (s, ^{L}**C$_{Ar}$2**), 135.0 (s, ^{L}**C$_{Ar}$4**), 134.6 (d, $^3J_{C,P}$ = 11 Hz, *m*-P-**C$_{Ar}$**), 133.3 (d, $^4J_{C,P}$ = 7 Hz, ^{L}**C$_{Ar}$16**), 131.0 (d, $^3J_{C,P}$ = 1 Hz, ^{L}**C$_{Ar}$1**-Se), 130.8 (d, $^4J_{C,P}$ = 3 Hz, *p*-P-**C$_{Ar}$**), 129.2 (d, $^1J_{C,P}$ = 61 Hz, P-**C$_{Ar}$**), 127.9 (d, $^2J_{C,P}$ = 11 Hz, *o*-P-**C$_{Ar}$**), 126.6 (s, ^{L}**C$_{Ar}$13**), 123.1 (s, ^{L}**C$_{Ar}$14**), 122.0 (d, $^4J_{C,P}$ = 1 Hz, ^{L}**C$_{Ar}$5**), 119.3 (s, ^{L}**C$_{Ar}$12**), 116.7 ($^5J_{C,P}$ = 1 Hz, ^{L}**C$_{Ar}$15**), 115.6 (s, ^{L}**C$_{Ar}$3**). ^{31}P NMR ($CDCl_3$, ppm): 8.1 (s), 8.2 (d, $^1J_{P,Pt}$ = 3719 Hz, $P^{\tilde{1}95}$Pt). ^{77}Se NMR ($CDCl_3$, ppm): 196.8 (d, $^2J_{Se,P}$ = 31 Hz). ^{195}Pt NMR ($CDCl_3$, ppm): –3675 (d, $^1J_{Pt,P}$ = 3772 Hz).

[Pt(L^{Te})(PPh_3)]. $[PtCl_2(PPh_3)_2]$ (80 mg, 0.1 mmol) and $\{HL^{Te}\}_2$ (52 mg, 0.08 mmol) were suspended in a degassed mixture of EtOH (1 mL) and CH_2Cl_2 (3 mL). The clear orange-red solution was heated to reflux and NEt_3 (1 drop) was added, which resulted in a color-change to dark red-brown. The heating was continued for 3 days. Then, the CH_2Cl_2 was distilled off and the remaining solution was cooled to room temperature. The addition of an excess of a 1:1 mixture of EtOH and hexane (ca. 60 mL) induced precipitation. The light red precipitate was filtered off and washed with EtOH, diethyl ether and hexane. The dark red powder was dried in vacuo. The product can be recrystallized by slow evaporation of a CH_2Cl_2/diethyl ether mixture. Dark red powder or orange-red needles. Yield: 43 mg (55 %).

Elemental analysis: Calculated for $C_{31}H_{24}NOPPtTe$: C 47.7, H 3.1, N 1.8 %; Found C 47.5, H 3.2, N 1.8 %. IR (cm^{-1}): $\tilde{\nu}$ = 3048 (w), 1605 (m) C=N, 1584 (m), 1569 (m), 1523 (m), 1482 (m), 1455 (m), 1435 (s), 1390 (m), 1366 (m), 1331 (m), 1263 (w), 1248 (w), 1216 (w), 1191 (w), 1170 (m), 1148 (s), 1127 (m), 1099 (s), 1047 (w), 1028 (m), 997 (w), 951 (vw), 931 (w), 839 (w), 801 (w), 738 (vs), 709 (sh), 693 (vs),

617 (sh), 610 (m), 580 (w), 556 (m), 538 (vs). ESI$^+$ MS (*m/z*): 781.0349 (calc. 798.0324) $[M]^+$, 798.0332 (calc. 798.0324) $[M + OH]^+$, 812.0551 (calc. 812.0481) $[M + OMe]^+$. ^{1}H NMR ($CDCl_3$, ppm): 8.9 (1H, d, $^4J_{H,P}$ = 12.65 Hz, **H17**CR=NR), 8.9 (dd, $^3J_{H,Pt}$ = 43.94 Hz, $^4J_{H,P}$ not determined due to overlap with the main signal of the aldiminic proton, **H17**CR=NR), 7.86–7.73 (7H, m, *m*-P-Ar**H**, ^{L}Ar**H15**), 7.54–7.39 (11H, m, 6 *o*-P-Ar**H**, 3 *p*-P-Ar**H**, ^{L}Ar**H2**, ^{L}Ar**H12**), 7.16–7.10 (2H, m, ^{L}Ar**H4**, ^{L}ArH**14**), 6.92 (1H, m, ^{L}Ar**H13**), 6.71–6.58 (2H, m, ^{L}Ar**H3**, ^{L}Ar**H5**). ^{13}C NMR ($CDCl_3$, ppm): 168.6 (s, ^{L}**C$_{Ar}$6**), 164.2 (s, H**C17**R=NR), 157.4 (d, $^3J_{C,P}$ = 4 Hz, ^{L}**C$_{Ar}$11**), 136.3 (s, ^{L}**C$_{Ar}$2**), 136.2 (s, ^{L}**C$_{Ar}$4**), 136.2 (d, $^4J_{C,P}$ = 1 Hz, ^{L}**C$_{Ar}$16**), 135.1 (d, $^3J_{C,P}$ = 11 Hz, *m*-P-**C$_{Ar}$**), 131.4 (d, $^4J_{C,P}$ = 3 Hz, *p*-P-**C$_{Ar}$**), 130.8 (d, $^1J_{C,P}$ = 62 Hz, P-**C$_{Ar}$**), 128.5 (d, $^2J_{C,P}$ = 11 Hz, *o*-P-**C$_{Ar}$**), 127.1 (s, ^{L}**C$_{Ar}$13**), 125.2 (s, ^{L}**C$_{Ar}$14**), 122.3 (d, $^4J_{C,P}$ = 1 Hz, ^{L}**C$_{Ar}$5**), 120.2 (s, ^{L}**C$_{Ar}$12**), 119.4 (d, $^5J_{C,P}$ = 1 Hz, ^{L}**C$_{Ar}$15**), 116.1 (s, ^{L}**C$_{Ar}$3**), 110.6 (d, $^3J_{C,P}$ = 6 Hz, ^{L}**C$_{Ar}$1**-Te). ^{31}P NMR ($CDCl_3$, ppm): 4.8 (s), 4.8 (d, $^1J_{P,Pt}$ = 3712 Hz, P^{195}Pt), 4.5 (d, *J* = 1559 Hz). ^{125}Te NMR ($CDCl_3$, ppm): 300.1 (d, $^2J_{Te,P}$ = 58 Hz). ^{195}Pt NMR ($CDCl_3$, ppm): –3895 (d, $^1J_{Pt,P}$ = 3651 Hz).

{[(HO)C$_6$H$_4$-(CHN$^+$H)-C$_6$H$_4$-TeI$_2$]·OPPh$_3$}. A solution of elemental iodine (25 mg, 0.1 mmol) in CH_2Cl_2 (2 mL) was added dropwise to a dry, degassed solution of $OPPh_3$ (28 mg, 0.1 mmol) and $\{HL^{Te}\}_2$ (32 mg, 0.05 mmol) in CH_2Cl_2 (4 mL). A red precipitate formed from the green-brown solution immediately. The mixture was stirred at room temperature for 3 h. The precipitate was filtered off and extracted with CH_2Cl_2 (3 × 4 mL), diethyl ether (10 mL) and hexane (10 mL). The combined filtrates and extract solutions were slowly evaporated. The formed black-violet crystals were filtered off, washed with diethyl ether and dried in vacuo. Black-violet blocks. Yield: 19 mg (22 %).

Elemental analysis: Calculated for $C_{31}H_{26}I_2NO_2PTe$: C 43.5, H 2.9, N 1.6 %; Found C 42.8, H 3.1, N 1.6 %. IR (cm^{-1}): $\tilde{\nu}$ = 3050 (m) N-H, 2324 (br) O-H, 1737 (br), 1624 (s) C=N, 1606 (s), 1584 (s), 1571 (s), 1502 (w), 1476 (w), 1434 (s), 1380 (m), 1360 (m), 1294 (w), 1242 (m), 1185 (m), 1160 (sh), 1141 (vs), 1120 (vs), 1086 (vs), 1069 (s), 1026 (m), 995 (vs), 944 (w), 905 (m), 876 (m), 852 (m), 784 (vw), 748 (vs), 722 (vs), 691 (vs), 632 (vw), 616 (w), 573 (w), 557 (m), 538 (vs). ESI$^+$ MS (*m/z*): 301.0600 (calc. 301.0758) $[OPPh_3 + Na]^+$, 579.1396 (calc. 579.1619) $[(OPPh_3)_2 + Na]^+$, 666.0842 (calc. 666.0695) $[M – 2HI – H + CH_3CN + Na]^+$, 857.2221 (calc. 857.2479) $[(OPPh_3)_3 + Na]^+$. ^{1}H NMR (CD_2Cl_2, ppm): 8.76 (1H, s, **H17**CR=NR), 8.38 (d, $^2J_{H,P}$ = 7.79 Hz, RO-**H1**···$OPPh_3$), 7.79–7.69 (21H, m, 6 *m*-P-Ar**H**, ^{L}Ar**H15**, 3 *p*-P-Ar**H**, 6 *o*-P-Ar**H**, ^{L}Ar**H2**, ^{L}Ar**H12**, ^{L}Ar**H5**, ^{L}ArH**14**, ^{L}Ar**H15**), 7.37 (1H, m, ^{L}Ar**H3**), 7.28 (1H, m, ^{L}Ar**H4**), 7.09 (1H, m, ^{L}Ar**H13**). ^{31}P NMR (CD_2Cl_2, ppm): 32.6 (s).

Deposition Numbers 2021656, 2021657, 2021658, 2021659, 2021660, 2021661 and 2021662 contain the supplementary crystallographic data for this paper. These data are provided free of charge by the joint Cambridge Crystallographic Data Centre and Fachinformationszentrum Karlsruhe Access Structures service www.ccdc.cam.ac.uk/structures.

Acknowledgments

This work was generously supported by the German Academic Exchange Service (DAAD, Germany) and the Coordenação de Aperfeiçoamento de Pessoal de Nível Superior (CAPES, Brazil). We also gratefully acknowledge the assistance of the Core Facility BioSupraMol supported by the DFG and the High-Performance-Computing (HPC) Centre of the Zentraleinrichtung für Datenverarbeitung (ZEDAT) of the Freie Universität Berlin for computational time and support. Open access funding enabled and organized by Projekt DEAL.

Keywords: Nickel · Palladium · Platinum · Selenolate · Tellurolate · Schiff bases · Reduction

[1] W. H. Hegazy, A. E.-D. M. Gaafar, *Am. Chem. Sci. J.* **2012**, *2*, 86–99.
[2] Z. H. Chohan, H. Pervez, A. Rauf, A. Scozzafava, C. T. Supuran, *J. Enzyme Inhib. Med. Chem.* **2002**, *17*, 117–122.
[3] N. I. al-Salim, W. R. McWhinnie, *Polyhedron* **1989**, *8*, 2769–2776.
[4] M. A. Arafath, F. Adam, M. R. Razali, L. E. A. Hassan, M. B. K. Ahamed, A. M. S. A. Majid, *J. Mol. Struct.* **2017**, *1130*, 791–798.
[5] E. A. Elzahany, K. H. Hegab, S. K. H. Khalil, N. S. Youssef, *Aust. J. Basic Appl. Sci.* **2008**, *2*, 210–220.
[6] P.-Y. Shi, Y.-H. Liu, S.-M. Peng, S.-T. Liu, *Organometallics* **2002**, *21*, 3203–3207.
[7] H. Motschi, C. Nusaumer, P. S. Pregosin, *Helv. Chim. Acta* **1980**, *63*, 2071–2086.
[8] N. Roy, S. Sproules, E. Bothe, T. Weyhermüller, K. Wieghardt, *Eur. J. Inorg. Chem.* **2009**, *2009*, 2655–2663.
[9] M. M. Tamizh, B. F. T. Cooper, C. L. B. Macdonald, R. Karvembu, *Inorg. Chim. Acta* **2013**, *394*, 391–400.
[10] M. Shabbir, Z. Akhter, I. Ahmad, S. Ahmed, M. Shafiq, B. Mirza, V. McKee, K. S. Munawar, A. R. Ashraf, *J. Mol. Struct.* **2016**, *1118*, 250–258.
[11] M. Shabbir, Z. Akhter, A. R. Ashraf, H. Ismail, A. Habib, B. Mirza, *J. Mol. Struct.* **2017**, *1149*, 720–726.
[12] M. M. Tamizh, K. Mereiter, K. Kirchner, B. R. Bhat, R. Karvembu, *Polyhedron* **2009**, *28*, 2157–2164.
[13] C. Manzur, C. Bustos, R. Schrebler, D. Carrillo, *Polyhedron* **1989**, *8*, 2321–2330.
[14] P. Raj, A. Singh, K. Kaur, T. Aree, A. Singh, N. Singh, *Inorg. Chem.* **2016**, *55*, 4874–4883.
[15] V. Kuchtanin, L. Kleščíková, M. Šoral, R. Fischer, Z. Růžičková, E. Rakovský, J. Moncol', P. Segl'a, *Polyhedron* **2016**, *117*, 90–96.
[16] *Cambridge Structural Database*, Release 5.40, November **2018**.
[17] B. Noschang Cabral, L. Kirsten, A. Hagenbach, P. C. Piquini, M. Patzschke, E. S. Lang, U. Abram, *Dalton Trans.* **2017**, *46*, 9280–9286.
[18] B. Noschang Cabral, *Doctoral* Thesis, Universidade Federal Santa Maria, **2017**.
[19] V. P. Ananikov, I. P. Beletskaya, G. G. Aleksandrov, I. L. Eremenko, *Organometallics* **2003**, *22*, 1414–1421.
[20] Gysling, H. J., *Ligand properties of organic selenium and tellurium compounds, in Organic Selenium and Tellurium Compounds: Volume 1*, 679–855, **1986**, (Eds.: S. Patai, Z. Rappoport), John Wiley & Sons, Inc., Chichester, UK. DOI: https://doi.org/https://doi.org/10.1002/9780470771761.ch18.
[21] R. Oilunkaniemi, R. S. Laitinen, M. Ahlgrén, *J. Organomet. Chem.* **2001**, *623*, 168–175.
[22] T. Chakraborty, K. Srivastava, H. B. Singh, R. J. Butcher, *J. Organomet. Chem.* **2011**, *696*, 2782–2788.
[23] P. K. Dutta, A. K. Asatkar, S. S. Zade, S. Panda, *Dalton Trans.* **2014**, *43*, 1736–1743.
[24] N. Ghavale, A. Wadawale, S. Dey, V. K. Jain, *Ind. J. Chem.* **2009**, *48A*, 1510–1514.
[25] B. Tirloni, C. N. Cechin, G. F. Razera, M. B. Pereira, G. M. de Oliveira, E. S. Lang, *Z. Anorg. Allg. Chem.* **2016**, *642*, 239–245.
[26] R. Kaur, S. C. Menon, S. Panda, H. B. Singh, R. P. Patel, R. J. Butcher, *Organometallics* **2009**, *28*, 2363–2371.
[27] D. Back, G. M. de Oliveira, E. S. Lang, *Polyhedron* **2015**, *85*, 565–569.
[28] B. Tirloni, E. S. Lang, G. M. de Oliveira, P. Piquini, M. Horner, *New J. Chem.* **2014**, *38*, 2394–2399.
[29] S. Kolay, M. Kumar, A. Wadawale, D. Das, V. K. Jain, *Dalton Trans.* **2014**, *43*, 16056–16065.
[30] M. Roca Jungfer, A. Hagenbach, E. S. Lang, U. Abram, *Eur. J. Inorg. Chem.* **2019**, *2019*, 4974–4984.
[31] R. Cargnelutti, E. S. Lang, P. Piquini, U. Abram, *Inorg. Chem. Commun.* **2014**, *45*, 48–50.
[32] C. Amatore, A. Jutand, M. A. M'Barki, *Organometallics* **1992**, *11*, 3009–3013.
[33] S. Ford, C. P. Morley, M. Di Vaira, *Inorg. Chem.* **2004**, *43*, 7101–7110.
[34] M. Risto, E. M. Jahr, M. S. Hannu-Kuure, R. Oilunkaniemi, R. S. Laitinen, *J. Organomet. Chem.* **2007**, *692*, 2193–2204.

[35] T. G. Appleton, M. A. Bennett, *Inorg. Chem.* **1978**, *17*, 738–747.
[36] R. J. Butcher, T. Chakravorty, H. B. Singh, *Acta Crystallogr., Sect. E.* **2012**, *68*, m141.
[37] M. Risto, R. Oilunkaniemi, R. S. Laitinen, M. Ahlgren, *Acta Crystallogr., Sect. E.* **2010**, *66*, m147.
[38] L. Kirsten, V. D. Schwade, L. Selter, A. Hagenbach, P. C. Piquini, E. S. Lang, U. Abram, *Eur. J. Inorg. Chem.* **2015**, *2015*, 3748–3757.
[39] L.-B. Han, F. Mirzaei, S. Shimada, *Heteroat. Chem.* **2018**, *29:e21463*, 1–4.
[40] R. Singh Chauhan, G. Kedarnath, A. Wadawale, D. K. Maity, J. A. Golen, A. L. Rheingold, V. K. Jain, *J. Organomet. Chem.* **2013**, *737*, 40–46.
[41] S. Kolay, A. Wadawale, S. Nigam, M. Kumar, C. Majumder, D. Das, V. K. Jain, *Inorg. Chem.* **2015**, *54*, 11741–11750.
[42] L.-B. Han, N. Choi, M. Tanaka, *J. Am. Chem. Soc.* **1997**, *119*, 1795–1796.
[43] L.-B. Han, S. Shimada, M. Tanaka, *J. Am. Chem. Soc.* **1997**, *119*, 8133–8134.
[44] P. J. Bonasia, J. Arnold, *J. Organomet. Chem.* **1993**, *449*, 147–157.
[45] R. G. Fortney-Zirker, W. Henderson, E. R. T. Tiekink, *Inorg. Chim. Acta* **2017**, *462*, 83–96.
[46] V. K. Jain, S. Kannan, R. Bohra, *Polyhedron* **1992**, *11*, 1551–1557.
[47] A. A. Pasynsky, Y. V. Torubaev, A. V. Pavlova, S. S. Shapovalov, I. V. Skabitsky, G. L. Denisov, *Russ. J. Coord. Chem.* **2014**, *40*, 527.
[48] T. Nakagawa, H. Seino, Y. Mizobe, *J. Organomet. Chem.* **2010**, *695*, 137–144.
[49] T. Nakagawa, H. Seino, S. Nagao, Y. Mizobe, *Angew. Chem. Int. Ed.* **2006**, *118*, 7922–7926; *Angew. Chem.* **2006**, *118*, 7922.
[50] M. M. Karjalainen, T. Wiegand, J. Mikko Rautiainen, A. Wagner, H. Gorls, W. Weigand, R. Oilunkaniemi, R. S. Laitinen, *J. Organomet. Chem.* **2007**, *836–837*, 17.
[51] D. M. Giolando, T. B. Rauchfuss, A. L. Rheingold, *Inorg. Chem.* **1987**, *26*, 1636–1638.
[52] S. A. Batten, J. C. Jeffery, L. H. Rees, M. D. Rudd, F. G. A. Stone, *J. Chem. Soc., Dalton Trans.* **1998**, 2839.
[53] C.-K. Hsieh, F.-C. Lo, G.-H. Lee, S.-M. Peng, W.-F. Liaw, *J. Chin. Chem. Soc.* **2000**, *47*, 103–107.
[54] J. J. Schneider, J. Kuhnigkh, C. Kruger, *Inorg. Chim. Acta* **1997**, *266*, 109–112.
[55] A. A. Pasynskii, S. S. Shapovalov, I. V. Skabitskii, O. G. Tikhonova, *Russ. J. Coord. Chem.* **2017**, *43*, 837–842.
[56] C.-H. Hsieh, I.-J. Hsu, C.-M. Lee, S.-C. Ke, T.-Y. Wang, G.-H. Lee, Y. Wang, J.-M. Chen, J.-F. Lee, W.-F. Liaw, *Inorg. Chem.* **2003**, *42*, 3925–3933.
[57] S. A. Yao, V. Martin-Diaconescu, I. Infante, K. M. Lancaster, A. W. Götz, S. DeBeer, J. F. Berry, *J. Am. Chem. Soc.* **2015**, *137*, 4993–5011.
[58] H. Sitzmann, D. Saurenz, G. Wolmershäuser, A. Klein, R. Boese, *Organometallics* **2001**, *20*, 700–705.
[59] S. S. Shapovalov, A. A. Pasynskii, I. V. Skabitskii, O. G. Tikhonova, A. V. Kolos, M. O. Grigor'eva, *Russ. J. Coord. Chem.* **2018**, *44*, 647–652.
[60] M. Brandl, A. Ebner, M. M. Kubicki, Y. Mugnier, J. Wachter, E. Vigier-Juteau, M. Zabel, *Eur. J. Inorg. Chem.* **2007**, *2007*, 994–1003.
[61] S. dos Santos, B. N. Cabral, U. Abram, E. S. Lang, *J. Organomet. Chem.* **2013**, *723*, 115–121.
[62] A. J. Londero, N. Ramirez, P. C. Piquini, U. Abram, E. S. Lang, *J. Organomet. Chem.* submitted.
[63] L. M. Venanzi, *J. Chem. Soc.* **1958**, 719–724.
[64] T. A. Stephenson, S. M. Morehouse, A. R. Powell, J. P. Heffer, G. Wilkinson, *J. Chem. Soc.* **1965**, 3632–3640.
[65] K. A. Jensen, *Z. Anorg. Allg. Chem.* **1936**, *229*, 242–251.
[66] A. A. Grinberg, Z. A. Razumova, *Zh. Prikl. Khim.* **1954**, *27*, 105.
[67] J. C. Bailar Jr., H. Itatani, *Inorg. Chem.* **1965**, *4*, 1618–1620.
[68] C. S. Radatz, D. Alves, P. H. Schneider, *Tetrahedron* **2013**, *69*, 1316–1321.
[69] L. Engman, D. Stern, I. A. Cotgreave, C. M. Andersson, *J. Am. Chem. Soc.* **1992**, *114*, 9737–9743.
[70] A. M. Deobald, L. R. S. de Camargo, G. Tabarelli, M. Hörner, O. E. D. Rodrigues, D. Alves, A. L. Braga, *Tetrahedron Lett.* **2010**, *51*, 3364–3367.
[71] R. K. Harris, E. D. Becker, S. M. Cabral de Menezes, P. Granger, R. E. Hoffman, K. W. Zilm, *Magn. Reson. Chem.* **2008**, *46*, 582–598.
[72] G. M. Sheldrick, *SADABS*, University of Göttingen, Germany, **1996**.
[73] P. Coppens, *The Evaluation of Absorption and Extinction in Single-Crystal Structure Analysis*, Crystallographic Computing, Copenhagen, Muksgaard, **1979**.
[74] G. M. Sheldrick, *Acta Crystallogr., Sect. A* **2008**, *64*, 112–122.
[75] G. M. Sheldrick, *Acta Crystallogr., Sect. C* **2015**, *71*, 3–8.
[76] *Diamond - Crystal and Molecular Structure Visualization* Crystal Impact - Dr. H. Putz & Dr. K. Brandenburg GbR, Bonn, Germany.
[77] M. J. Frisch, G. W. Trucks, H. B. Schlegel, G. E. Scuseria, M. A. Robb, J. R. Cheeseman, G. Scalmani, V. Barone, B. Mennucci, G. A. Petersson, H. Nakatsuji, M. Caricato, X. Li, H. P. Hratchian, A. F. Izmaylov, J. Bloino, G. Zheng, J. L. Sonnenberg, M. Hada, M. Ehara, K. Toyota, R. Fukuda, J. Hasegawa, M. Ishida, T. Nakajima, Y. Honda, O. Kitao, H. Nakai, T. Vreven, J. A. Montgomery Jr., J. E. Peralta, F. Ogliaro, M. Bearpark, J. J. Heyd, E. Brothers, K. N. Kudin, V. N. Staroverov, R. Kobayashi, J. Normand, K. Raghavachari, A. Rendell, J. C. Burant, S. S. Iyengar, J. Tomasi, M. Cossi, N. Rega, J. M. Millam, M. Klene, J. E. Knox, J. B. Cross, V. Bakken, C. Adamo, J. Jaramillo, R. Gomperts, R. E. Stratmann, O. Yazyev, A. J. Austin, R. Cammi, C. Pomelli, J. W. Ochterski, R. L. Martin, K. Morokuma, V. G. Zakrzewski, G. A. Voth, P. Salvador, J. J. Dannenberg, S. Dapprich, A. D. Daniels, Ö. Farkas, J. B. Foresman, J. V. Ortiz, J. Cioslowski, D. J. Fox, *Gaussian 09, Revision B.01*, Gaussian, Inc., Wallingford CT, **2016**.
[78] M. J. Frisch, G. W. Trucks, H. B. Schlegel, G. E. Scuseria, M. A. Robb, J. R. Cheeseman, G. Scalmani, V. Barone, G. A. Petersson, H. Nakatsuji, X. Li, M. Caricato, A. Marenich, J. Bloino, B. G. Janesko, R. Gomperts, B. Mennucci, H. P. Hratchian, J. V. Ortiz, A. F. Izmaylov, J. L. Sonnenberg, D. Williams-Young, F. Ding, F. Lipparini, F. Egidi, J. Goings, B. Peng, A. Petrone, T. Henderson, D. Ranasinghe, V. G. Zakrzewski, J. Gao, N. Rega, G. Zheng, W. Liang, M. Hada, M. Ehara, K. Toyota, R. Fukuda, J. Hasegawa, M. Ishida, T. Nakajima, Y. Honda, O. Kitao, H. Nakai, T. Vreven, K. Throssell, J. A. Montgomery Jr., J. E. Peralta, F. Ogliaro, M. Bearpark, J. J. Heyd, E. Brothers, K. N. Kudin, V. N. Staroverov, T. Keith, R. Kobayashi, J. Normand, K. Raghavachari, A. Rendell, J. C. Burant, S. S. Iyengar, J. Tomasi, M. Cossi, J. M. Millam, M. Klene, C. Adamo, R. Cammi, J. W. Ochterski, R. L. Martin, K. Morokuma, O. Farkas, J. B. Foresman, and D. J. Fox, *Gaussian 09*, *Revision A.02*, Gaussian, Inc., Wallingford CT, **2016**.
[79] *GaussView*, Version 6, Roy Dennington, Todd A. Keith, and John M. Millam, Semichem Inc., Shawnee Mission, KS, **2016**.
[80] S. H. Vosko, L. Wilk, M. Nusair, *Can. J. Phys.* **1980**, *58*, 1200–1211.
[81] A. D. Becke, *J. Chem. Phys.* **1993**, *98*, 5648–5652.
[82] C. Lee, W. Yang, R. G. Parr, *Phys. Rev. B* **1988**, *37*, 785–789.
[83] P. J. Hay, W. R. Wadt, R. Willard, *J. Chem. Phys.* **1985**, *82*, 299–310.
[84] A. Bergner, M. Dolg, W. Küchle, H. Stoll, H. Preuß, *Mol. Phys.* **1993**, *80*, 1431–1441.
[85] W. J. Pietro, E. S. Blurock, R. F. Hout, W. J. Hehre, D. J. DeFrees, R. F. Stewart, *Inorg. Chem.* **1981**, *20*, 3650–3654.
[86] M. M. Francl, W. J. Pietro, W. J. Hehre, J. S. Binkley, M. S. Gordon, D. J. DeFrees, J. A. Pople, *J. Chem. Phys.* **1982**, *77*, 3654–3665.
[87] M. S. Gordon, J. S. Binkley, J. A. Pople, W. J. Pietro, W. J. Hehre, *J. Am. Chem. Soc.* **1982**, *104*, 2797–2803.
[88] P. C. Hariharan, J. A. Pople, *Theor. Chim. Acta* **1973**, *28*, 213–222.
[89] W. J. Hehre, R. Ditchfield, J. A. Pople, *J. Chem. Phys.* **1972**, *56*, 2257–2261.
[90] V. A. Rassolov, M. A. Ratner, J. A. Pople, P. C. Redfern, L. A. Curtiss, *J. Comput. Chem.* **2001**, *22*, 976–984.
[91] R. Ditchfield, W. J. Hehre, J. A. Pople, *J. Chem. Phys.* **1971**, *54*, 724–728.
[92] K. L. Schuchardt, B. T. Didier, T. Elsethagen, L. Sun, V. Gurumoorthi, J. Chase, J. Li, T. L. Windus, *J. Chem. Inf. Model.* **2007**, *47*, 1045–1052.
[93] S. Grimme, *Chem. Eur. J.* **2012**, *18*, 9955–9964. (DOI: https://doi.org/10.1002/chem.201200497).
[94] R. Paton, I. Funes-Ardoiz; https://zenodo.org/badge/latestdoi/16266/bobbypaton/GoodVibes; DOI: https://doi.org/10.5281/zenodo.3346166.
[95] T. Lu, F. Chen, *J. Comput. Chem.* **2012**, *33*, 580–592. (http://sobereva.com/multiwfn).

Received: August 6, 2020